

## Chemical Logic Gates

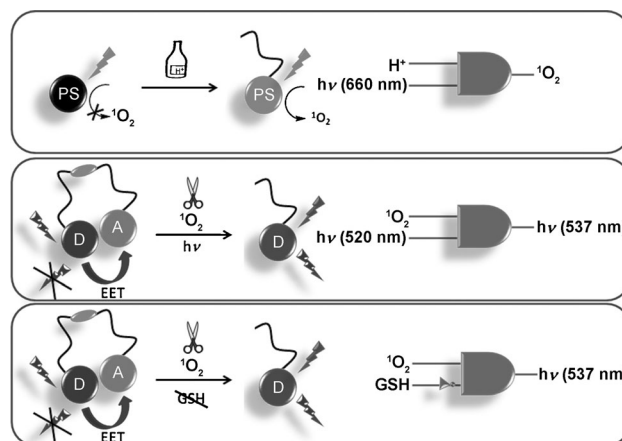
# Cascading of Molecular Logic Gates for Advanced Functions: A Self-Reporting, Activatable Photosensitizer\*\*

Sundus Erbas-Cakmak and Engin U. Akkaya\*

The complexity of biochemical reaction networks usually arises from the cascade of reactions that control or are controlled by other reactions in the network. This enables signal relay between functional biological modules and generates intricate emerging processes. The same analogy is also applicable to silicon-based logic operations. Indeed, complex digital computational processes show similar levels of dependency on series of simple logic operations, from which sophisticated algorithms can be effectively produced.

Chemical logic gates, on the other hand, are already able to perform quite complex tasks,<sup>[1]</sup> as exemplified by multiplexer/demultiplexer,<sup>[2]</sup> flip-flop logics,<sup>[3]</sup> subtracter/adder,<sup>[4]</sup> or keypad-lock<sup>[5]</sup> systems. Smart oligonucleotide-based constructs playing simple games such as Tic-Tac-Toe have been reported.<sup>[6]</sup> Physical cascading (concatenation and integration) of a series of simple logic gates with chemical or electronic communication in between has also been described.<sup>[7]</sup> Nevertheless, the de novo assembly of a practical and functional logic construct that relies on the conveyance of signals between each independent module, or between logic gates as a whole, has not been demonstrated thus far. Herein, we propose a cascade of two chemical logic gates that concatenates an acid-activatable photosensitizer and an activity-reporting moiety through a singlet-oxygen-mediated information relay.

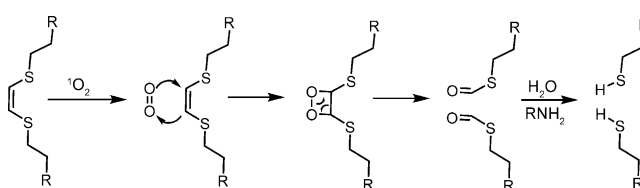
To enable such an intentional and physical cascading with modular logic gates, photodynamic action and chemical probe moieties were considered. As the output of photodynamic action is singlet oxygen ( $^1\text{O}_2$ ), we aimed at developing a reaction that senses this output and thus reports the activity of the first action. The working principles for the individual logic operations are shown in Scheme 1. The first logic gate includes an AND logic operation; 660 nm light and acid are applied as inputs, and the singlet oxygen produced on photosensitization is the output. Considering a likely practical potential, the slightly acidic microenvironment of a tumor tissue<sup>[8]</sup> was targeted with the use of an acid-responsive photosensitizer (PS), as the  $\text{p}K_{\text{a}}$  of the micelle-embedded



**Scheme 1.** Working principles for the individual AND and INHIBIT logic gates.

photosensitizer has to be optimal for its use in such an application. The excitation of the PS at the irradiation wavelength (660 nm) is more pronounced for its protonated form as a result of the blue shift in the absorption spectrum. This is our pH-activatable photosensitizer (Scheme 1).

The second logic gate can be considered either as an AND gate that uses  $^1\text{O}_2$  (the output of the first logic operation) and 520 nm light as an input, or as an INHIBIT gate with  $^1\text{O}_2$  and glutathione (GSH) as the inputs. Glutathione concentrations have been reported to be much higher in cancer cells than in normal cells. The design of the second logic gate is such that two energy-transfer modules are attached to one another using a  $^1\text{O}_2$ -reactive linker. The linker is (*Z*)-1,2-bis(alkylthio)ethane, which was reported to have very high reaction rates with  $^1\text{O}_2$ , and which is easily synthesized.<sup>[9]</sup> The reaction of this linker with  $^1\text{O}_2$  is shown in Scheme 2. Following the initial addition of  $^1\text{O}_2$  to the double bond, an unstable dioxethane is formed, and spontaneous decomposition of this intermediate produces *S*-alkyl methanethioate. In aqueous solutions and in the presence of amines, this compound has been reported to be easily hydrolyzed to the corresponding thiols.<sup>[9]</sup>



**Scheme 2.** The reaction of  $^1\text{O}_2$  with electron-rich olefins.<sup>[9]</sup>

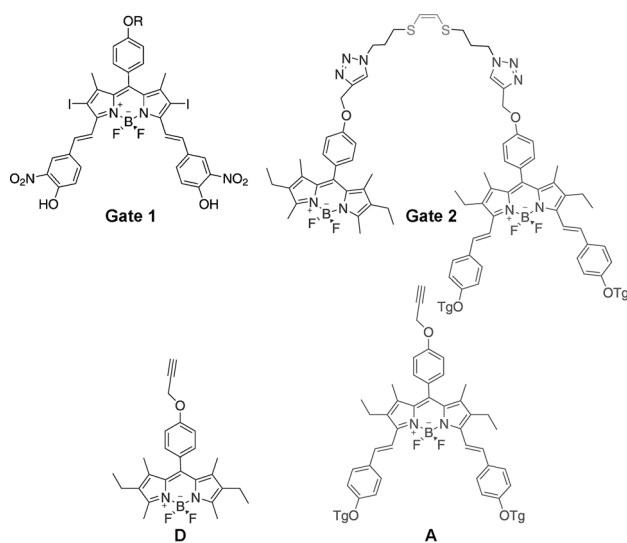
[\*] Dr. S. Erbas-Cakmak, Prof. Dr. E. U. Akkaya  
UNAM-Institute of Materials Science and Nanotechnology  
Bilkent University, Ankara, 06800 (Turkey)  
E-mail: eua@fen.bilkent.edu.tr

Prof. Dr. E. U. Akkaya  
Department of Chemistry, Bilkent University  
Ankara, 06800 (Turkey)

[\*\*] S.E.-C. thanks TUBITAK for a scholarship, and the authors thank Mr. Yusuf Cakmak for fruitful discussions.

Supporting information for this article is available on the WWW under <http://dx.doi.org/10.1002/anie.201306177>.

Following the cleavage of the linker, excitation of the donor results in bright emission, because the acceptor is not in the vicinity to act as an energy sink. Two energy-transfer modules and two molecular logic gate constructs are shown in Scheme 3.



**Scheme 3.** Independent logic gates and energy donor (D) and acceptor (A) modules. Tg = methoxytriethyleneglycol.

The acidic nature of tumor tissue has been known for some time, but the pH difference between healthy and malignant regions is not very large.<sup>[10]</sup> The pH is usually above six and even close to neutrality for most tumors. Thus, the pH-activatable PS was selected accordingly, keeping possible biological applications in mind. With rational modifications, the  $pK_a$  of the photosensitizer was chemically adjusted to slightly acidic values, so that the micellar (Cremophor-EL) photosensitizer (Gate 1, Scheme 3; see also the Supporting Information, Figure S1) has a  $pK_a$  of 6.92 in aqueous solutions. Electronic absorption spectra of the gates and the energy-transfer modules in tetrahydrofuran (THF) are given in Figure 1. The absorption maximum of the deprotonated form of the micellar photosensitizer (Gate 1) moves from 649 nm to 720 nm in aqueous solution (Figure S2). Furthermore, the compound is essentially non-emissive in this form (Table 1; see also Figure S3).

The spectral shift in absorption and other possible deactivation processes that are active at alkaline and neutral pH facilitate the selective sensitization of the PS in acidic media. Figure 2 shows the singlet-oxygen-generation activity of the micelle-embedded Gate 1 in slightly acidic (pH ca. 6.0) and slightly basic (pH ca. 7.5) aqueous solutions, which was detected by the selective bleaching of 2,2'-anthracene-9,10-diylbis(methylene)dimalonic acid by the produced  $^1O_2$ . As expected, the results indicate that singlet oxygen is efficiently generated only under irradiation with 660 nm light in acidic media. Using the change in trap absorption in the presence of Gate 1, an AND logic is constructed (Figure 3). The percentage decrease in trap absorption at 378 nm was determined as a measure of  $^1O_2$ -generation ability, and the threshold rate

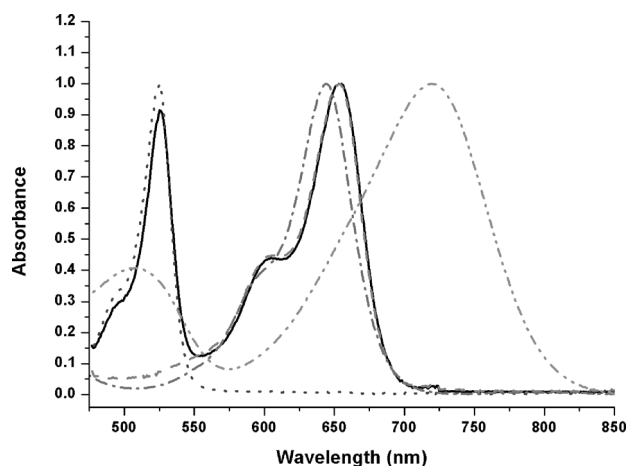


**Figure 1.** Normalized electronic absorption spectra of Gate 2 (—), A (---), D (.....), Gate 1 (-.-.-), and Gate 1 in the presence of piperidine (—) in THF.

**Table 1:** Photophysical characterization of Gates 1 and 2 and modules D and A.

Compound	$\lambda_{\text{abs}}$ [nm]	$\epsilon$ [ $M^{-1} \text{cm}^{-1}$ ]	$\lambda_{\text{F}}$ [nm]	$\phi_{\text{F}}^{[a]}$ [ $\lambda_{\text{exc}}$ (nm)]	$\tau_{\text{F}}^{[b]}$ [ns]
Gate 1	645 <sup>[a]</sup>	40 000	667	0.13	1.2
	720	30 000	—	0.00	—
Gate 2	525	85 000	537	0.14	3.5
	654	93 000	670	0.56	4.4
D	525	70 000	535	0.96	4.9
A	654	76 000	670	0.50	4.5

[a] Values were obtained in THF. [b] Values were obtained in THF with piperidine as an additive. [c] The following reference compounds were used for quantum-yield calculations: For emission-band peaking at 537 nm, Rhodamine 6G (water,  $\phi_{\text{F}} = 0.95$ ,  $n = 1.333$ ) was used, and for emission-band peaking at 670 nm, Cresyl Violet (MeOH,  $\phi_{\text{F}} = 0.66$ ,  $n = 1.329$ ) was used.

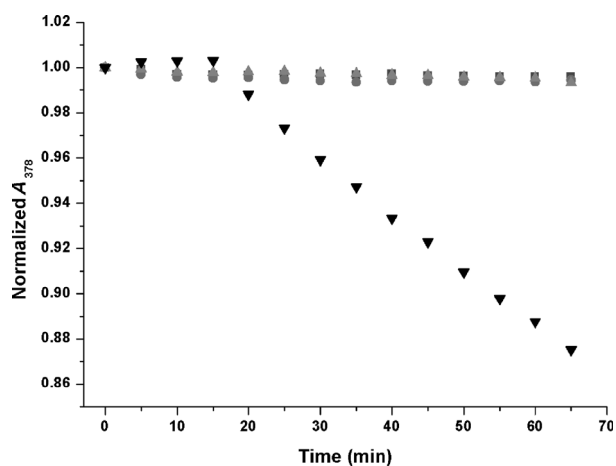


**Figure 2.** Relative  $^1O_2$ -generation efficiency of micellar Gate 1 (7.5  $\mu\text{M}$ ) in aqueous solutions in the presence (▼) or absence (▲) of acid, detected by the absorption decrease of the trap at 378 nm. The changes in the trap absorption in slightly basic (■) and acidic (●) solutions (pH = ca. 7.5 and 6.0, respectively) are also shown. During the first 15 min, the samples were kept in the dark, and for the following 50 min, the samples were irradiated with 660 nm light using an LED array.

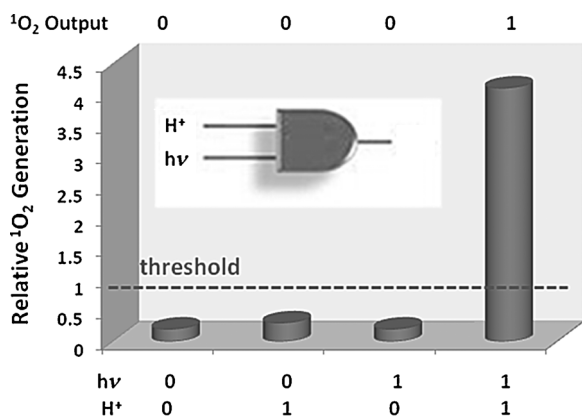


**Figure 3.** AND logic construct of the photosensitizer (Gate 1). The output ( $^1\text{O}_2$ ) is measured as a percentage decrease in trap absorption within 15 min (in the dark or with 660 nm irradiation). The inputs are 660 nm light and acid. The threshold was set at 1.

was set at 1. Taking the values obtained by incubation for 15 min in the dark, or under irradiation with 660 nm light, in either slightly acidic or basic aqueous solutions, the AND logic shown in Figure 3 was obtained. The output levels clearly demonstrate that the photosensitizer is activated in acidic media with essentially no dark reaction.

The second part of the logic-gate cascade was developed using the  $^1\text{O}_2$  produced (the output of the first AND gate) and either 520 nm light or GSH as inputs. To analyze the cascade, two compounds (corresponding to Gates 1 and 2) were embedded together within a micelle in a mole ratio of approximately 1:1. The concentrations were estimated by comparison of the absorption values with the THF absorptivities. Micellar constructs of Gates 1 and 2 were prepared for the analysis of the second logic gate and  $\text{D}_2\text{O}$  was used to enhance the lifetime of  $^1\text{O}_2$ .

A comparison of the emission spectra of Gate 2 with that of the energy-transfer module shows that the emission of the excitation energy transfer (EET) of the donor part **D** at 537 nm is considerably quenched in Gate 2. This was further supported by a decrease in the quantum yield of the donor emission from 0.96 to 0.14 (Figure 4, Table 1). On the other hand, the EET acceptor module **A** cannot be excited at 520 nm to produce an emission at 670 nm, whereas Gate 2 shows intense emission at this wavelength upon excitation at 520 nm (Figure 4b). Both of these spectroscopic results indicate an efficient EET process between the modules with a calculated efficiency of 85.0%. An efficiency of less than one unit in this process is probably due to poor spectral overlap between the donor and acceptor moieties. Excitation spectra also confirm that the acceptor emission is a result of the excitation of both donor and acceptor moieties (Figure 5). In contrast, excitation spectra of the acceptor **A** do not display any peaks around 524 nm, when emission at 670 nm followed.

As the PS produces singlet oxygen only in the presence of acid, acidic conditions are interpreted as the presence of  $^1\text{O}_2$  at the second logic gate. Liberation of the EET donor upon the reaction of Gate 2 with  $^1\text{O}_2$  is expected. The samples kept

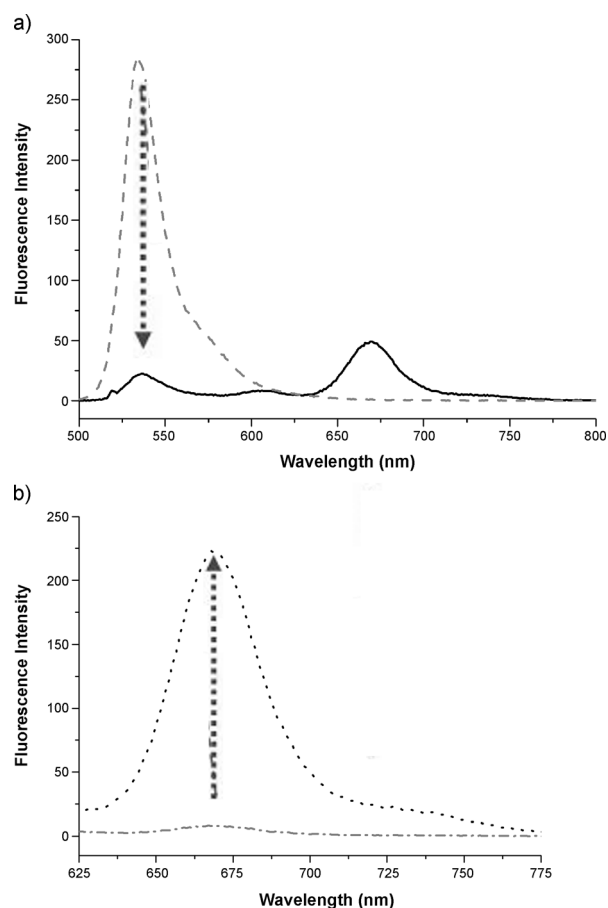


**Figure 4.** Comparison of the emission spectra of a) equally absorbing Gate 2 (—) and the EET donor (**D**, ---) excited at 520 nm, and b) of Gate 2 (•••••) and the EET acceptor (**A**, -•-•-) excited at the same wavelength in THF.

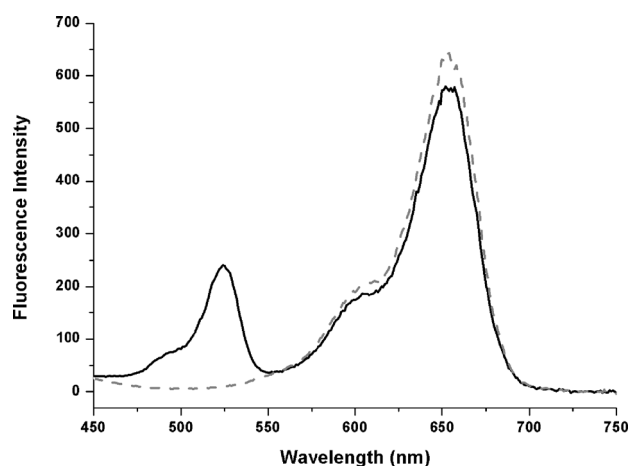


**Figure 5.** Comparison of the excitation spectra of the equally absorbing compounds **A** (-•-•-) and Gate 2 (—) for emission at 670 nm in THF.

in the dark do not display any change in the emission of the EET donor module of Gate 2 at 537 nm (Figure S4). Likewise, under slightly basic conditions, no significant change in the emission is observed because  $^1\text{O}_2$  is not generated

efficiently under these conditions (Figures S5 and S6). However, when acid is present to activate the PS, a more than twofold increase in the emission intensity of the donor at 537 nm indicates that it has been detached from the energy acceptor module; the increase in the emission seems to reach almost a constant value (Figure 7). Nevertheless, the final

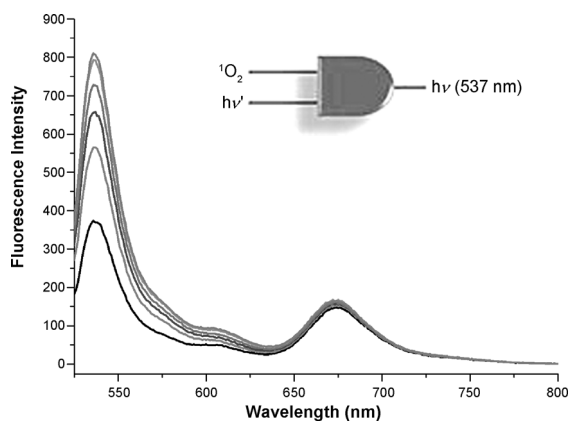


**Figure 6.** Changes in the emission spectra of Gate 2 (0.75  $\mu\text{m}$ ) in the presence of Gate 1 (0.75  $\mu\text{m}$ ) in  $\text{D}_2\text{O}$  upon irradiation with 660 nm light for 50 min. The spectra of the samples were recorded under excitation at 520 nm at 10 min intervals.

quantum yield is smaller than the quantum yield of the free EET donor **D**, and the excitation spectra do not display a significant decrease for the donor part (Figure S7). By comparing the quantum yields of the free EET donor **D** and Gate 2 after light irradiation (660 nm) for 50 min, a cleavage of 18% can be estimated. This is already enough to obtain an intense fluorescence output (Figure 6). The quantum yield of the donor emission within the micellar construct increases from 0.14 to 0.29, and the increase in the emission almost seems to level out (Figure 7). This could indicate that the EET

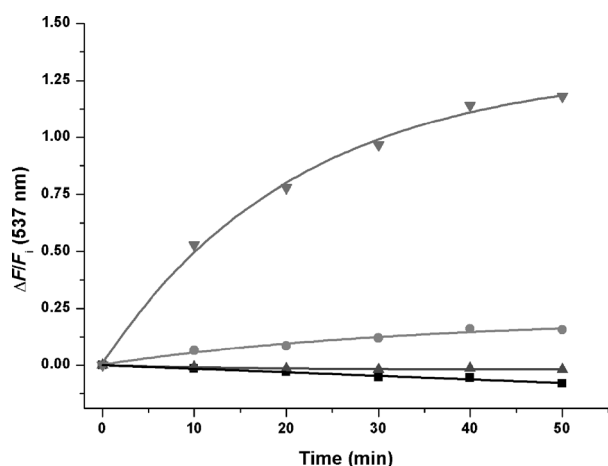


**Figure 7.** Changes in the fluorescence at 537 nm of the micellar Gates 1 and 2 in  $\text{D}_2\text{O}$  for different combinations of conditions: dark and basic (■), light and basic (●), dark and acidic (▲), and light and acidic (▼). Light was supplied by a 660 nm LED source. All four samples were excited at 520 nm.

process is still effective to some extent, owing to Gate 2 molecules that had remained uncleaved thus far. This result may be due to a decrease in the amount of oxygen dissolved in the solution after a certain time, which leads to a decrease in the reaction rate. In actual biological media, the oxygen flow within blood and tissue is usually under homeostasis, and thus essentially constant.

The overall results for the fluorescence enhancement in the presence of acid or 660 nm light are given in Figure 7. The singlet-oxygen-mediated fluorescence enhancement at 537 nm is apparently more pronounced in the presence of  $^1\text{O}_2$ , which is efficiently produced in the presence of 660 nm light in acidic aqueous media.

To make sure that the resultant increase is not solely due to irradiation, or to test the stability of Gate 2 under irradiation with the same experimental conditions, a micelle containing only this compound (Gate 2) was tested in aqueous solutions. The results show that the increase in the emission of the donor in the absence of the photosensitizer is essentially zero (Figure S8), which indicates that the main contributor to the enhancement at 537 nm is  $^1\text{O}_2$ .

Considering all of the above results, the second AND logic was constructed. As an excitation at 520 nm is required for the second logic gate, the absence of light at this wavelength corresponds to a zero output (no excitation). The results are depicted in Figure 8, with an assigned threshold value of 0.3.

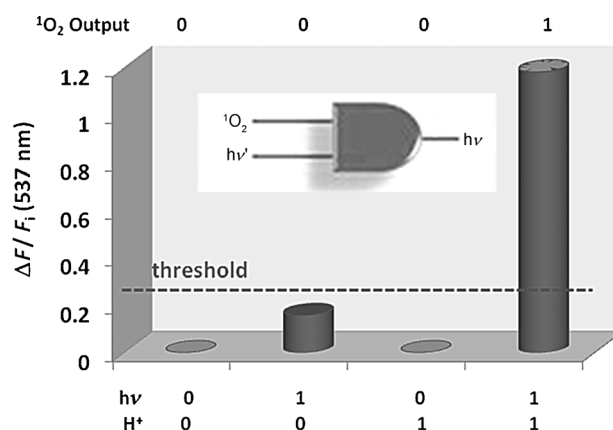


**Figure 8.** Construction of the second AND logic gate with light (520 nm) and acid as the inputs; the output is reported as a fractional change in the emission intensity at 537 nm. The threshold was set at 0.3.

Although light has been applied as an input in a number of logic-gate designs in the literature, this input may seem trivial, as the excitation is required anyway for any fluorescence process. Therefore, an alternative input was chosen for the second gate, namely glutathione. High levels of this molecule lead to resistance against photodynamic therapy (PDT) because of its properties as a singlet oxygen scavenger.<sup>[11]</sup> To suppress the PDT-deactivating property of GSH at high concentrations, researchers use chemicals to decrease the biological production of this molecule.<sup>[12]</sup> Herein, GSH was used as the input because of its role as a singlet oxygen

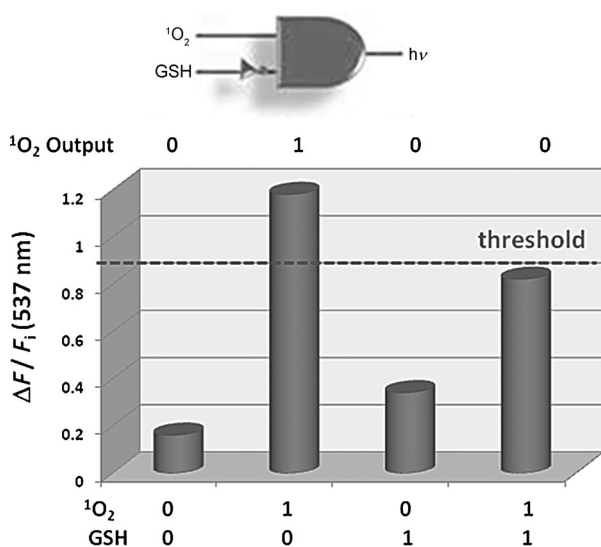


**Figure 9.** INHIBIT logic gate with the inputs  $^1\text{O}_2$  and GSH; the output is emission at 537 nm.

scavenger. For efficient impact on the  $^1\text{O}_2$  produced, the GSH level should be low. The results of a fluorescence enhancement at 537 nm under different conditions are shown in Figure S9.

The results in Figures S9 and 9 show that the presence of GSH interferes with fluorescence enhancement. This data may be interpreted as follows: GSH acts as a  $^1\text{O}_2$  scavenger and decreases the  $^1\text{O}_2$  level; thus, the rate of fluorescence enhancement is diminished. The lack of a quantitative decrease in the fluorescence enhancement may be due to limited diffusion of GSH to the interior of the micelle within the duration of experiment (50 min). However, an appropriate choice of threshold still allows the construction of an INHIBIT logic gate.

In conclusion, we were able to develop a modular cascade of independently functioning logic gates (Figure 10), and a logical construct with a higher function was thus obtained. An AND logic gate was used to control the activity of a PS with acid and light (Gate 1). The output of this gate, which is  $^1\text{O}_2$ , was used by another logic gate, either another AND gate or an INHIBIT gate, depending on the choice of input. By means of this concatenation, the two gates were designed to communicate with each other, such that the activity of a pH-activatable PS was monitored by the increase in the emission of a fluorescent reporter within the same micellar structure. This result supports the idea that molecular logic gates are

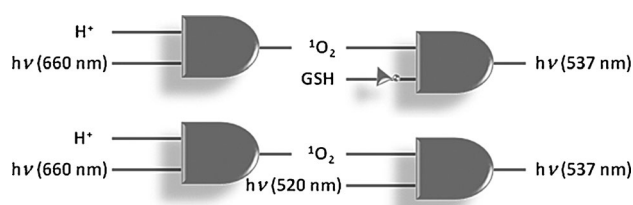


**Figure 10.** Two different logic-gate cascades. Two functional logic-gate modules are coerced to work together, yielding useful information about the rate of singlet oxygen production.

likely to find their first convincing application in a health-related niche. Further work along these lines is expected to produce such information-processing and smart therapeutic agents.

Received: July 16, 2013

Published online: September 12, 2013

**Keywords:** energy transfer · fluorescence · photodynamic therapy · photosensitizers · singlet oxygen

- [1] a) A. Credi, *Angew. Chem.* **2007**, *119*, 5568–5572; *Angew. Chem. Int. Ed.* **2007**, *46*, 5472–5475; b) J. Andréasson, U. Pischel, *Chem. Soc. Rev.* **2010**, *39*, 174–188; c) K. Szacilowski, *Chem. Soc. Rev.* **2008**, *108*, 3481–3548; d) S. Kou, H. N. Lee, D. van Noort, K. M. K. Swamy, S. H. Kim, J. H. Soh, K.-M. Lee, S.-W. Nam, J. Yoon, S. Park, *Angew. Chem.* **2008**, *120*, 886–890; *Angew. Chem. Int. Ed.* **2008**, *47*, 872–876.
- [2] a) J. Andréasson, S. D. Straight, S. Bandyopadhyay, R. H. Mitchell, T. A. Moore, D. Gust, *Angew. Chem.* **2007**, *119*, 976–979; *Angew. Chem. Int. Ed.* **2007**, *46*, 958–961; b) M. Amelia, M. Baroncini, A. Credi, *Angew. Chem.* **2008**, *120*, 6336–6339; *Angew. Chem. Int. Ed.* **2008**, *47*, 6240–6243; c) E. Perez-Inestrosa, J. M. Montenegro, D. Collado, R. Suau, *Chem. Commun.* **2008**, 1085–1087; d) S. Erbas-Cakmak, O. A. Bozdemir, Y. Cakmak, E. U. Akkaya, *Chem. Sci.* **2013**, *4*, 858–862.
- [3] a) G. de Ruiter, L. Motiei, J. Choudhury, N. Oded, M. E. van der Boom, *Angew. Chem.* **2010**, *122*, 4890–4893; *Angew. Chem. Int. Ed.* **2010**, *49*, 4780–4783; b) P. Remón, M. Balter, S. Li, J. Andréasson, U. Pischel, *J. Am. Chem. Soc.* **2011**, *133*, 20742–20745.
- [4] a) D. H. Qu, Q. C. Wang, Q. H. Tian, *Angew. Chem.* **2005**, *117*, 5430–5433; *Angew. Chem. Int. Ed.* **2005**, *44*, 5296–5299; b) M. Semeraro, A. Credi, *J. Phys. Chem. C* **2010**, *114*, 3209–3214; c) D. Margulies, G. Melman, A. Shanzer, *J. Am. Chem. Soc.* **2006**, *128*, 4865–4871.
- [5] D. Margulies, C. E. Felder, G. Melman, A. Shanzer, *J. Am. Chem. Soc.* **2007**, *129*, 347–354.
- [6] M. N. Stojanovic, D. Stefanovic, *Nat. Biotechnol.* **2003**, *21*, 1069–1074.
- [7] a) G. de Ruiter, E. Tartakovski, N. Oded, M. E. van der Boom, *Angew. Chem.* **2010**, *122*, 177–180; *Angew. Chem. Int. Ed.* **2010**, *49*, 173–176; b) V. Balzani, A. Credi, M. Venturi, *ChemPhysChem* **2003**, *4*, 49–59; c) R. Guliyev, S. Ozturk, Z. Kostereli, E. U. Akkaya, *Angew. Chem.* **2011**, *123*, 10000–10005; *Angew. Chem. Int. Ed.* **2011**, *50*, 9826–9831; d) T. Gupta, M. E. van der Boom, *Angew. Chem.* **2008**, *120*, 2292–2294; *Angew. Chem. Int. Ed.* **2008**, *47*, 2260–2262; e) T. Gupta, M. E. van der Boom, *Angew. Chem.* **2008**, *120*, 5402–5406; *Angew. Chem. Int. Ed.* **2008**, *47*, 5322–5326; f) S. Silvi, E. C. Constable, C. E. Housecroft, J. E. Beves, E. L. Dunphy, M. Tomasulo, F. M. Raymo, A. Credi, *Chem. Eur. J.* **2009**, *15*, 178–185; g) S. Silvi, E. C. Constable, C. E. Housecroft, J. E. Beves, E. L. Dunphy, M. Tomasulo, F. M. Raymo, A. Credi, *Chem. Commun.* **2009**, 1484–1486.
- [8] M. G. Vander Heiden, L. C. Cantley, C. B. Thompson, *Science* **2009**, *324*, 1029–1033.
- [9] A. Rotaru, A. Mokhir, *Angew. Chem.* **2007**, *119*, 6293–6296; *Angew. Chem. Int. Ed.* **2007**, *46*, 6180–6183.
- [10] R. J. Gillies, N. Raghunand, G. Karczmar, Z. Bhujwala, *J. Magn. Reson. Imaging* **2002**, *16*, 430–450.
- [11] T. P. Devasagayam, A. R. Sundquist, P. Mascio, S. Kaiser, H. Sies, *J. Photochem. Photobiol. B* **1991**, *9*, 105–116.
- [12] F. Jiang, L. Lilge, M. Belcuig, G. Singh, J. Grenier, Y. Li, M. Chopp, *Lasers Surg. Med.* **1998**, *23*, 161–166.